Research Article GU J Sci, Part A, 11(2): 407-418 (2024) 10.54287/gujsa.1475116

Gazi University
Journal of Science
PART A: ENGINEERING AND INNOVATION
http://dergipark.org.tr/gujsa

Effect of ZrO_2 on Radiation Permeability Properties of Polypropylene

Zübeyde ÖZKAN[1,2*] Berkay ÇAKIR[3] Seda Gürgen AVŞAR[3] Emir OLÇAY[3] Uğur GÖKMEN[3]

[1] Gazi University, Institute of Science and Technology, Ankara, Türkiye
[2] Gazi University, Institute of Science and Technology, Department of Advanced Technologies, Ankara, Türkiye
[3] Gazi University, Institute of Science and Technology, Department of Metallurgical and Materials Engineering, Ankara, Türkiye

Keywords

Polypropylene (PP)

ZrO2

Gamma Shielding

Neutron Composite

Abstract

The study investigates the radiation permeability properties including mass attenuation coefficient (MAC), linear attenuation coefficient (LAC), tenth value layer (TVL), half value layer (HVL), fast neutron cross section (FNRC), and mean free path (MFP) of polypropylene (PP) polymer, as well as the produced polymer matrix composites (PP+5% ZrO2, PP+10% ZrO2, PP+15% ZrO2). The studied materials were examined by considering their effect on radiation permeability against gamma and neutron radiation. Additionally, powder size, Archimedes principle (density), XRD, DSC, ATR, and DTA-TG analyses were performed. According to the radiation permeability results of the studied four materials, PP + 15% ZrO2 was found to have the highest LAC values, while PP was found to have the lowest LAC values. The FNRC values of the PP, PP+5% ZrO2, PP+10% ZrO2, and PP+15% ZrO2 materials were found to be 10.038 cm-1, 12.651 cm-1, 15.002 cm-1, and 17.091 cm-1, respectively. The most suitable material for gamma and neutron shielding was found to be 15% ZrO2 reinforced material.

Cite

Özkan, Z., Çakır, B., Avşar, S. G., Olçay, E., & Gökmen, U. (2024). Effect of ZrO2 on Radiation Permeability Properties of Polypropylene. *GU J Sci, Part A*, *11*(2), 407-418. doi:10.54287/gujsa.1475116

Author ID (ORCID Number)

0000-0003-2901-7749	Zübeyde ÖZKAN
0009-0001-5500-9438	Berkay ÇAKIR
0009-0008-9991-7236	Seda Gürgen AVŞAR
0009-0009-5257-6929	Emir OLÇAY
0000-0002-6903-0297	Uğur GÖKMEN

Article Process

Submission Date	29.04.2024
Revision Date	22.05.2024
Accepted Date	05.06.2024
Published Date	28.06.2024

1. INTRODUCTION

With the development of technology, energy demand has been rising with each passing day because of the increase in consumption. Thanks to nuclear power plants, it is possible to generate power in any quantity and at any time in line with demand. Therefore, the number of nuclear power plants has been increasing rapidly across the world. Nuclear power plants, like everything else, have several advantages, as well as some disadvantages. Any leak or explosion causes irreversible damage that will affect nature and human health for many years. As a result of radiation spreading to the environment, it affects not only the immediate surroundings of the nuclear power plant but also areas kilometers away from the power plant. As a result of the Chernobyl disaster that occurred on April 26, 1986, Bulgaria, Türkiye, Romania, etc. they were affected by radioactive substances spread throughout the countries. Therefore, radiation shielding is crucial for nuclear power plants (Akman et al., 2022; Szondy et al., 2024). Having a short wavelength, gamma rays emit high-frequency electromagnetic radiation. Since they are uncharged, neutron particles are not affected by Coulomb forces and do not interact with the nucleus. As a result of this, they have a higher penetration depth. Any leak in a nuclear power plant might pose severe health risks for living beings. It might result in hair loss, cataracts, gene damage, cancer, and even mortality in living beings (Tyagi et al., 2021; Ardiansyah et al., 2023; Aldawood et al., 2024). As a result, radiation shielding material is very important for human health and nature. Recently, Alzahrani et al. (2022), Malidarre et al. (2021), Kamislioglu (2021), and several

*Corresponding Author, e-mail: zubeydeozkan@gazi.edu.tr

other researchers have carried out many studies on materials to offer an alternative radiation shielding material that can eliminate the negative aspects of the shielding material currently used.

In this study, recyclable polypropylene (PP) material was used among polymer materials used for different purposes. In this way, as a result of the recycling of materials that have completed their intended use, their usability as gamma and fast neutron shielding material, which is a new field, has been investigated. Polymer matrix composite materials designed by adding ZrO_2 ceramic material at varying rates of 5-10-15% into the PP polymer matrix; the linear attenuation coefficient (LAC), mass attenuation coefficient (MAC), half value thickness (HVL), tenth value thickness (TVL), mean free distance (MFP) and fast neutron cross section (FNRC) parameters were examined and the radiation transmittance results against gamma and neutron radiations were analyzed. In addition, density, XRD, ATR, DSC and DTA-TG analyses of the PP material and SEM-EDS analyses of the ZrO_2 ceramic material, which provide information on powder grain size analysis and microstructural properties, were carried out.

2. MATERIALS AND METHOD

The powder size of the ZrO_2 ceramic powder used was dimensional utilizing Malvern Mastersizer 3000, which is a laser diffraction particle size analyzer. In addition, the microstructure of the material was examined under the SEM microscope to understand the powder grain shape, which is important in determining the production parameters. Then the XRD analyses of the PP were performed. Table 1 shows the chemical composition of the studied materials in the radiation permeability analysis. The melting point and vaporization temperature are crucial parameters in terms of radiation shielding. This is because the degradation of the radiation shielding material's chemical structure is very important for its resistance against radiation. Therefore, ATR, DSC, and DTA-TG analyses were performed on the studied PP polymer materials.

Table 1. *Chemical composition of the materials*

Name of the sample	Composition
S0	PP
S5	PP+5% ZrO_2
S10	PP+10% ZrO_2
S15	PP+15% ZrO_2

The gamma and neutron permeability analyses of polymer composites were performed by employing Phy-x/PSD (Şakar et al., 2020). The LAC and MAC which provide significant details about the material's shielding feature against radiation, are very prominent in the selection of shielding material. LAC (μ), which is the fraction of attenuated radiation in an energy beam per unit thickness of material, is obtained by utilising the Beer-Lambert law (Equation 1). MAC, on the other hand, is obtained by taking into account the density of the material in absorbing the incoming radiation. It is a measure of the possible interaction between photon and matter. The MAC value is given by divide the LAC value by the material intensity, as shown in Equation 2, where I_o, I, and x are the intensity of the radiation on the material, the intensity of the radiation passing through the material and the thickness of the material (cm), respectively

$$I = I_o e^{-\mu x} \tag{1}$$

$$\mu_m = \frac{\mu}{\rho} \tag{2}$$

HVL, MFP and TVL are very important parameters as they are utilizing to specify the thick of the radiation shielding material to be used. HVL indicates the thickness at which the shielding material decreases the incident radiation by half the intensity, while TVL indicates the thickness at which it reduces the incident radiation by 90% in centimeters. The mean distance traveled between two successive collisions by an incoming photon is specified by MFP. These parameters are calculated using Equations 3-4-5. FNRC is significant in terms of the absorption of fast neutrons. FNRC is calculated in centimeters by employing Eq. 6 (Kılıçoğlu & Tekin, 2020; Kavun et al., 2022).

GU J Sci, Part A 11(2) 407-418 (2024) 10.54287/gujsa.1475116

$$HVL = \frac{\ln(2)}{\mu} \tag{3}$$

$$TVL = \frac{\ln(10)}{\mu} \tag{4}$$

$$MFP = \frac{1}{\mu} \tag{5}$$

$$\sum_R = \sum_i \rho_i \left(\sum R/\rho\right)_i \tag{6}$$

3. RESULTS AND DISCUSSION

The average density of the studied PP, which was measured by Archimedes' principle, was found to be approximately 0.77 g/cm^3. Figure 1 shows the powder grain size distribution of the ZrO_2 ceramic powder used in the study. Dv (90), Dv (50), and Dv (10) values of the ZrO_2 ceramic powder were found to be 38.6 µm, 18.0 µm, and 3.46 µm, respectively. In Figure 2, it can be seen that the ZrO_2 ceramic powder has an angular shape at x1000 magnification. When the SEM image is examined, Dv (90), Dv (50) and Dv (10) differences in the powder grain size distribution are seen.

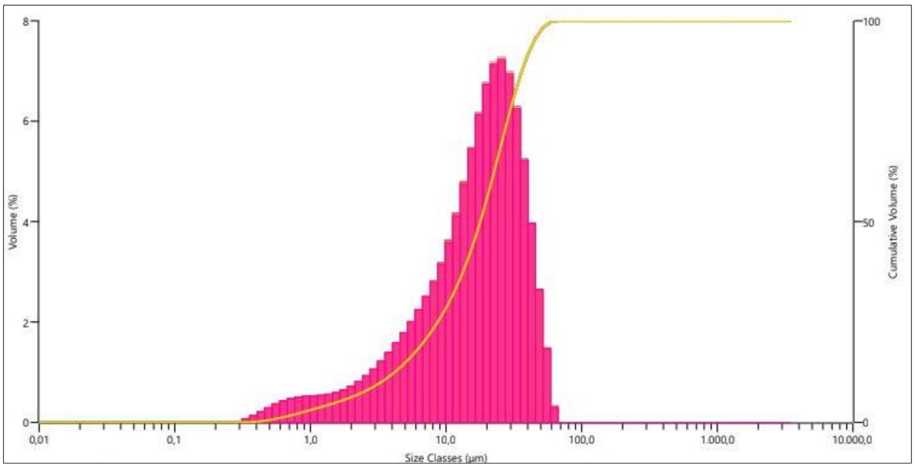

Figure 1. *Grain size distribution of the ZrO_2 ceramic powder*

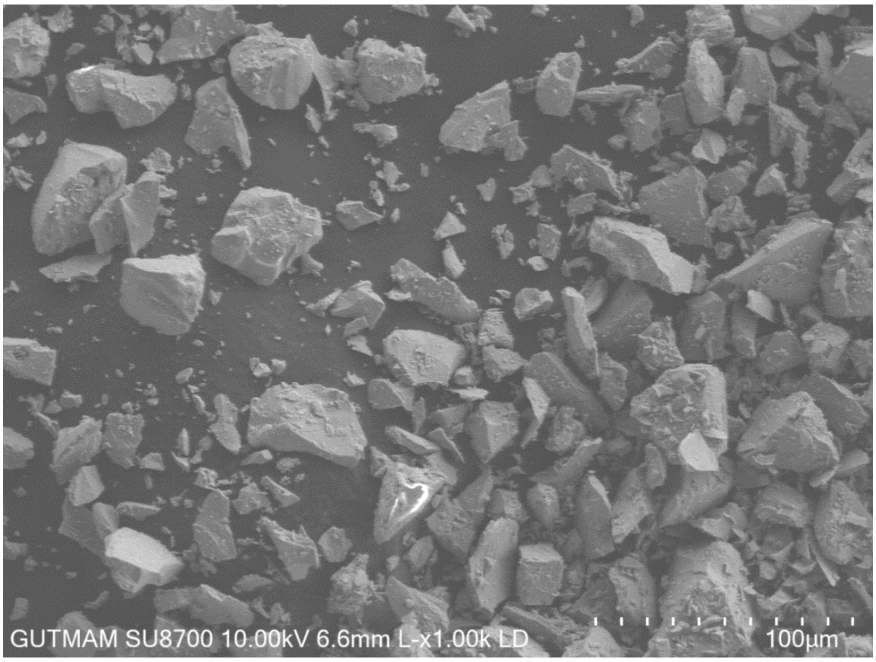

Figure 2. *SEM of the ZrO_2 ceramic powder*

Figure 3 presents the XRD analysis of PP, as well as the characteristic peaks with (hkl) Miller indices of the material. XRD analyzes of PP material were analyzed at 2θ° between 10º-90º. At 2θ°, the PP material gives peaks of (011), (040), (130), (111), and (060) to the crystal planes at about 14.3°, 17.2°, 18.7°, 21.3°, and 25.5°, respectively. The peaks of the XRD spectrum curve are also consistent with those of PP reported in the literature (Akinci et al., 2007; Mingliang et al., 2007). In addition, the crystallinity rate of the studied material was found by measuring the ratio of the entire area under the curve (Figure 3) to the crystal peak areas, using the equation given in Equation 7, and was calculated as 82.24%.

$$\%Crystallinity = \frac{A_{crystal}}{A_{curve}} \, x \, 100 \tag{7}$$

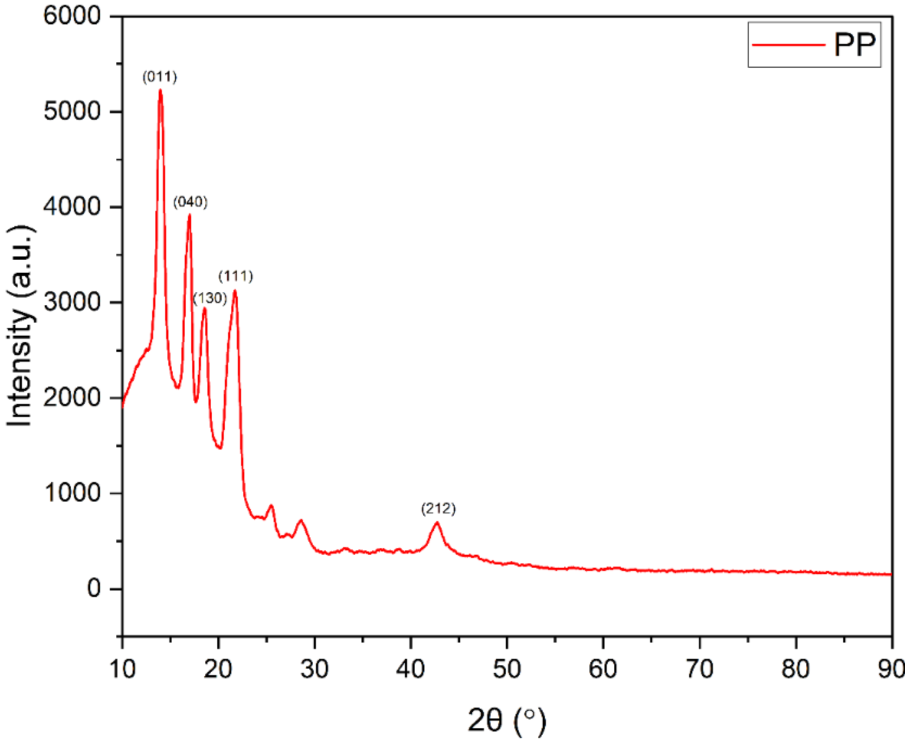

Figure 3. *XRD spectrum of the polypropylene*

Isotactic PP, a widely used commercial polymer, may have a simple chemical composition, but its self-assembly behavior and crystal structures are surprisingly complex. The type of polymer significantly affects semi-crystalline polymers' properties, including crystal thicknesses and crystallinity levels. The morphology of crystals is also greatly affected by thermo-mechanical processes (Labour et al., 2001; Akinci et al., 2007). In polymeric materials, the crystallization rate and amorphous regions change the materiel's thermal, physical, and mechanical characteristics (Akinci et al., 2007). Pure PP can usually be obtained in the following crystal shapes; α (monoclinic)γ (orthorhombic), and β (trigonal) as well as smectic mesophase, an intermediate state between amorphous and ordered phases. As it is the most stable state in terms of thermodynamic conditions, α state is the most commonly used form of PP in industry. Also, the melting point of isotactic polypropylene (iPP) is around 160–165 °C, which is relatively higher than other variations (Papageorgiou et al., 2012).

In Figure 4, the DSC spectrum of polypropylene was analyzed between 25°C - 250°C with increasing temperature at 10°C per minute. Multiple endothermic peaks occur at 136°C and 168°C, depending on the process involved in various fusion transitions. The main peak is observed at 168°C. Recrystallization or rearrangement of some crystallized fractions are the primary reasons for these multiple endothermic reactions (Cho et al., 1999). According to the TGA and DSC analysis results, it is observed that the melting point varies between 168°C and 172°C. In Figure 5, the DTA spectrum of polypropylene was analyzed between 25°C - 600°C with increasing temperature at 10°C per five minutes. Additionally, thermal decomposition of PP material begins around 453°C.

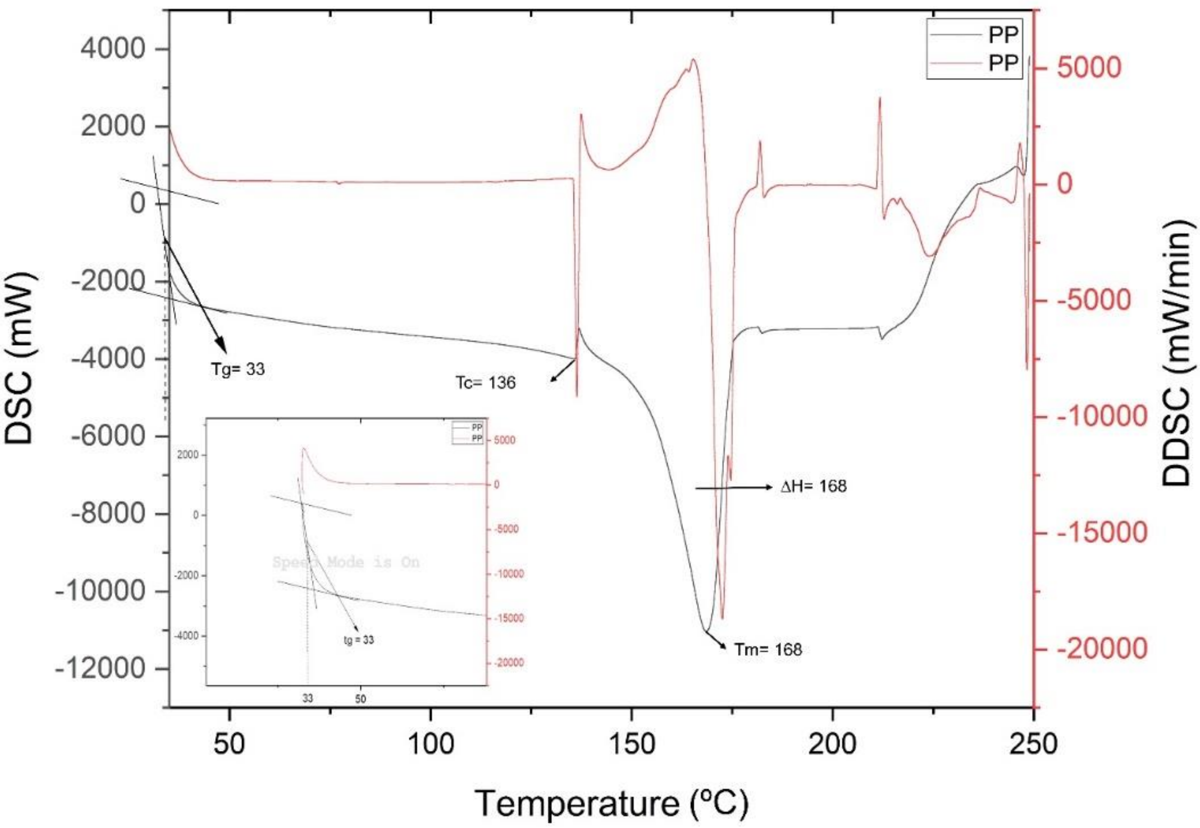

Figure 4. *DSC analysis of polypropylene*

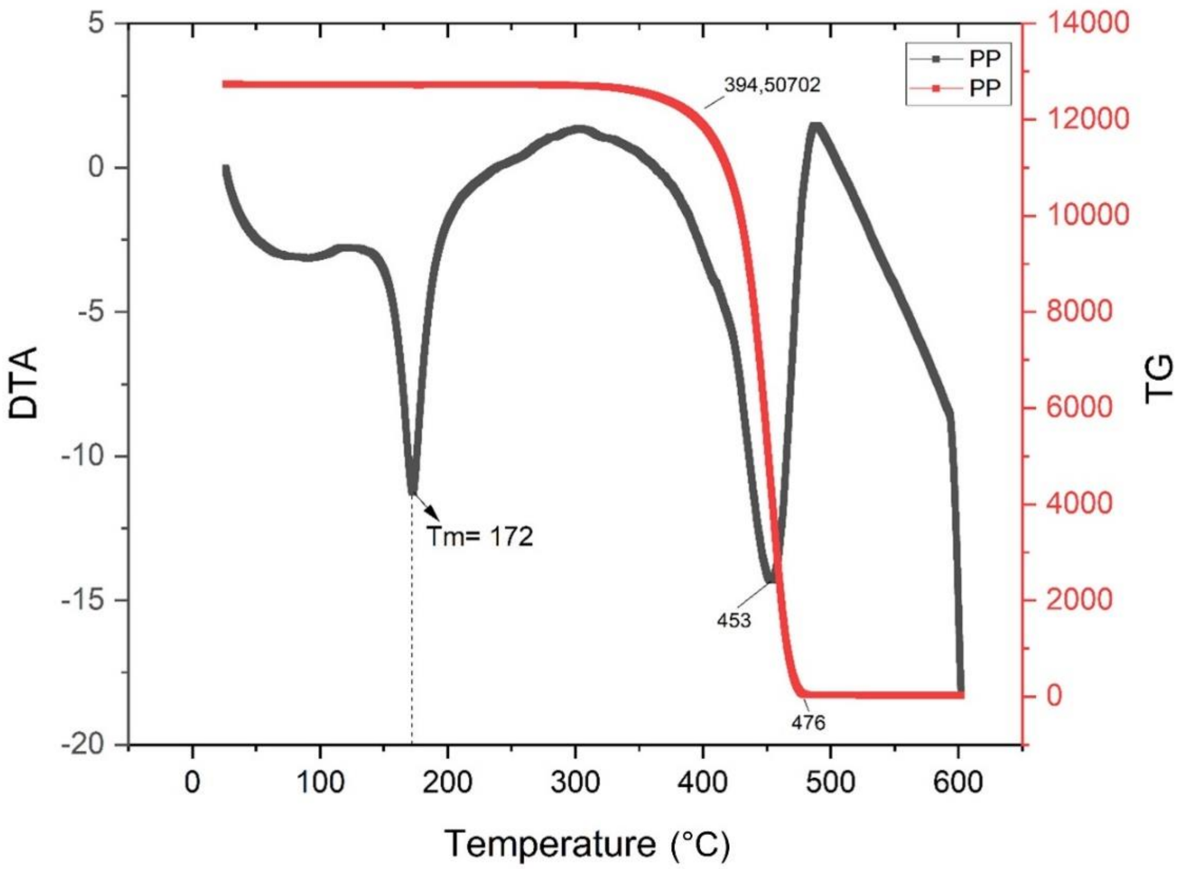

Figure 5. *DTA-TGA analysis of polypropylene*

ATR analysis PP material was analyzed at wavelengths of 550 cm^{-1} -4000 cm^{-1}. Figure 6 shows the spectrum of the PP material and the absorption peaks, which are consistent with those reported by the previous studies. In the isotactic polypropylene spectrum, the methylene group arises between the range from 1445 cm^{-1} to 1485 cm^{-1} while the methyl group originates between 430 cm^{-1} and 1470 cm^{-1} or between 1365 cm^{-1} and 1395 cm^{-1}. In spectrum, such peaks show 1451 cm^{-1} and 1377 cm^{-1}, respectively. The peak around 2915 cm^{-1} was linked to CH band vibration. The pure PP spectrum also contains characteristic peaks at 840, 1000, and 1170 cm^{-1}. These characteristic curves are observed at 1170, 997, and 840 cm^{-1}; however, they are not clearly detachable owing to the smoothing process (Krylova & Dukštienė, 2013).

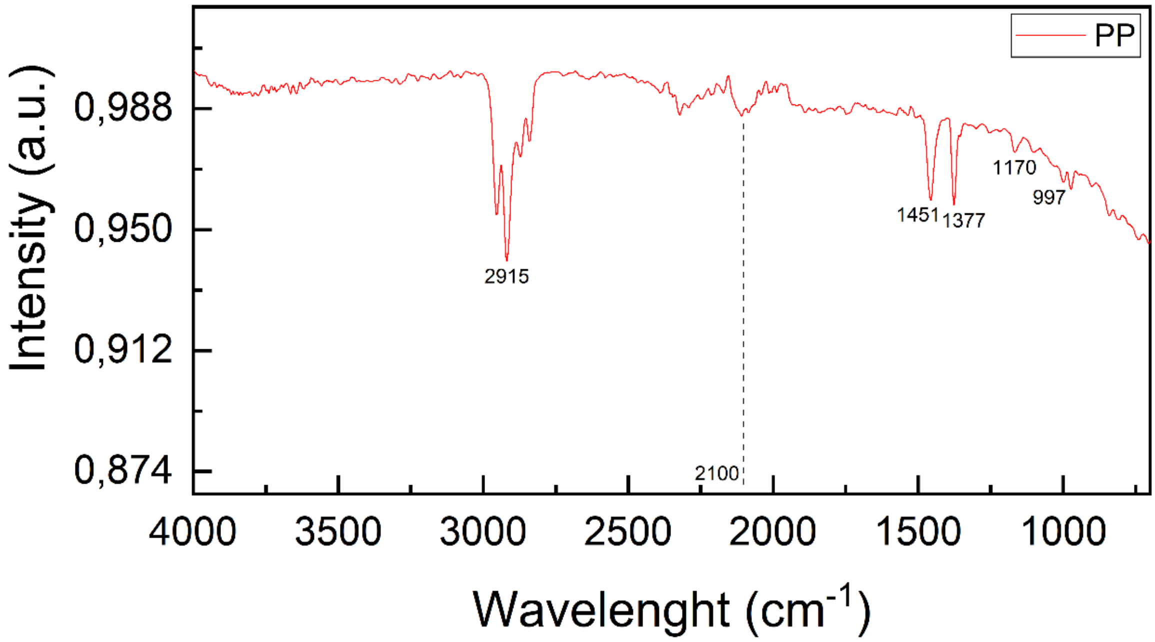

Figure 6. *ATR spectrum of polypropylene*

According to the LAC values (Figure 7), all studied samples have lower LAC figures with the increase in energy. It is observed that the radiation absorption abilities of materials are higher in the low energy range. The addition of 5% ZrO_2 in PP leads to a two-fold rise in the LAC worth of the PP polymer material. This is mainly because the ZrO_2 material is a high-density ceramic and contains elements with much higher atomic numbers compared to PP. The sample's LAC value increases depending on the increase in the proportion of the ZrO_2 addition. The photoelectric effect (PE) occurs dominantly in the of 0.005888 MeV<E<0.511 MeV. In this energy region, the PP, PP+5% ZrO_2, PP+10% ZrO_2, and PP+15% ZrO_2 materials exhibit the following ranges of the LAC values: 777.564 cm^{-1}–7.764 cm^{-1}, 2179.104 cm^{-1}–10.025 cm^{-1}, 4134.525 cm^{-1}–12.344 cm^{-1}, and 6643.827 cm^{-1}–14.633 cm^{-1}, respectively. At the energy of 0.662 MeV (^{137}Cs), where Compton scattering (CS) is predominant, PP, PP+5% ZrO_2, PP+10% ZrO_2, and PP+15% ZrO_2 materials get LAC values of 6.859 cm^{-1}, 8.947 cm^{-1}, 11.001 cm^{-1}, and 13.021 cm^{-1}, respectively. The studied polymer composites' LAC values are observed to get higher figures with the increase in the proportion of the ZrO_2 addition.

Figure 8 reveals that the MAC and LAC curves of the materials exhibit similar behaviors. While the variation in the studied materials' MAC values is more evident in the low photon energy regions, the variation in the samples' MAC values is closer to each other in the high photon energy region. This is because the materials have more interaction with photons and, accordingly, the absorption amount is higher at lower photon energies. In other words, it is due to the weaker ability of materials to absorb photons at high photon energies. For the energy level of 0.723 MeV (^{131}I), where CS is dominant, PP, PP+5% ZrO_2, PP+10% ZrO_2 and PP+15% ZrO_2 materials have the MAC values of 8.464 cm^2/g, 8.395 cm^2/g, 8.326 cm^2/g, and 8.256 cm^2/g, respectively. MAC values of the materials show well stability in the energy region after 2 MeV, where pair production predominantly occurs. At a photon energy of 2 MeV, the MAC values of PP, PP+5% ZrO_2, PP+10% ZrO_2, and PP+15% ZrO_2 materials are 5.064 cm^2/g, 5.023 cm^2/g, 4.981 cm^2/g, and 4.939 cm^2/g, respectively.

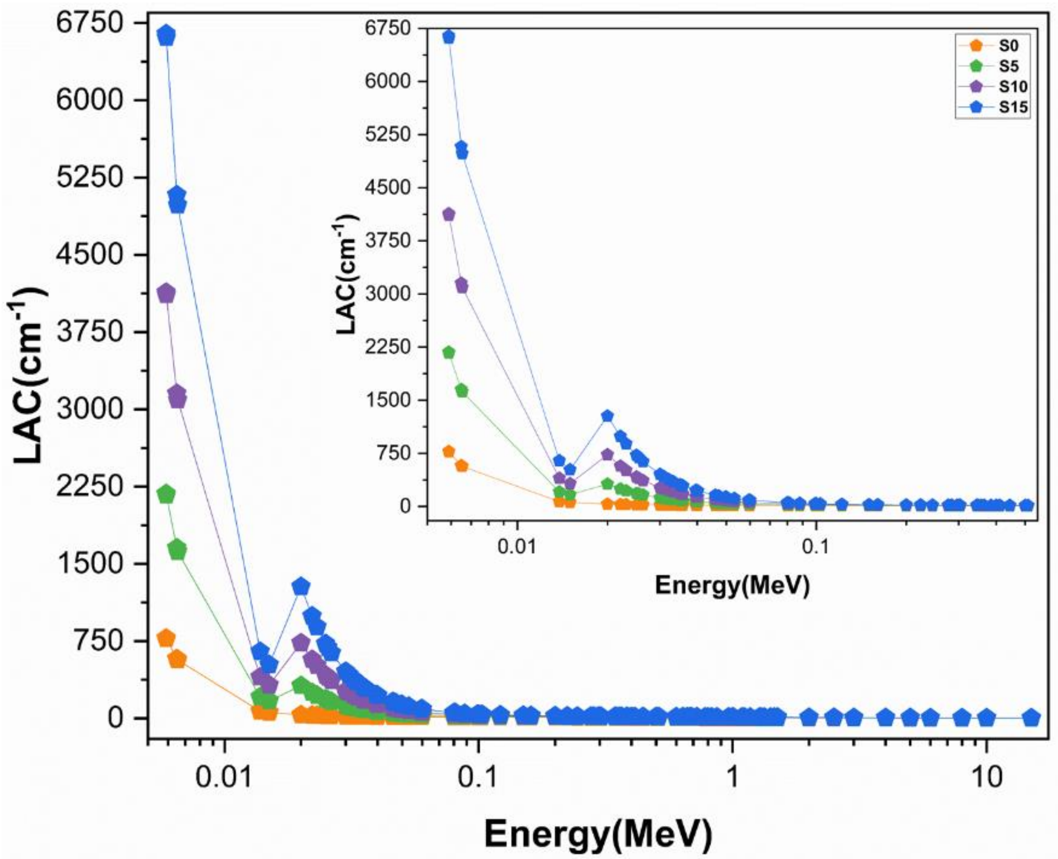

Figure 7. LAC values of the samples

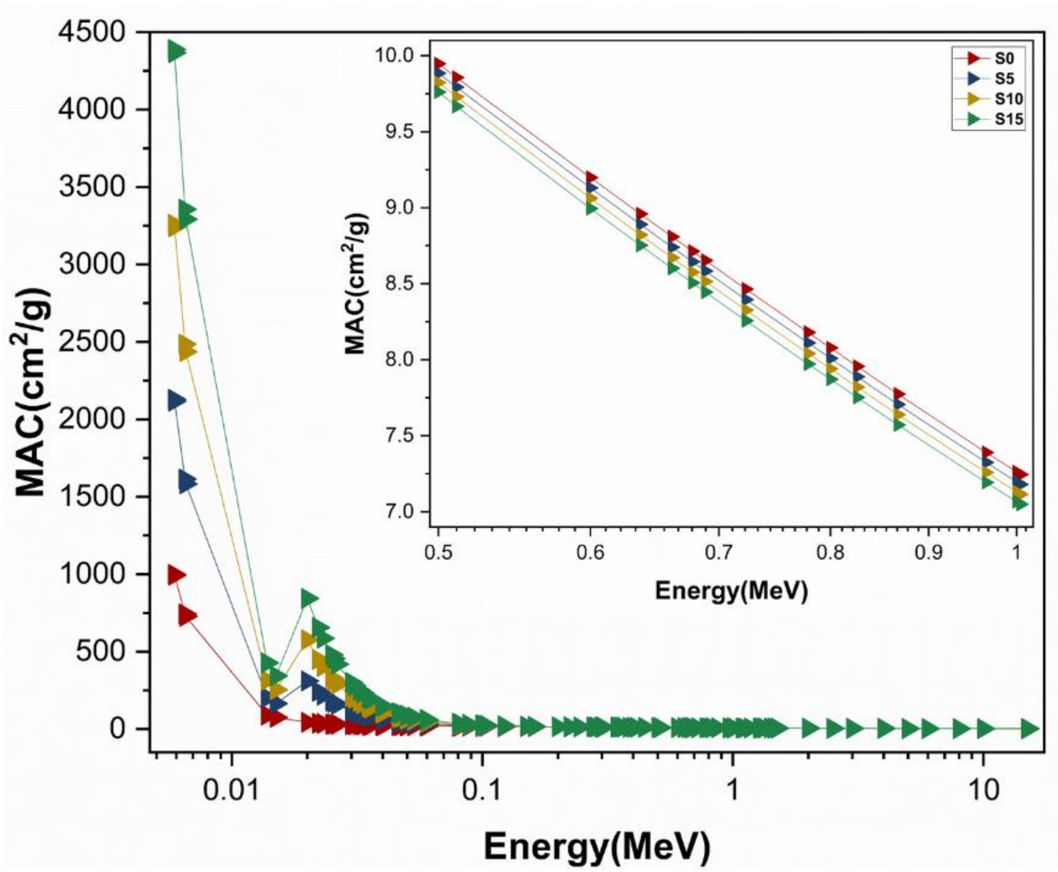

Figure 8. MAC values of the samples

GU J Sci, Part A 11(2) 407-418 (2024) 10.54287/gujsa.1475116

Considering the HVL plot of the studied materials, the HVL values get lower figures due to the higher absorption of the materials at low energies (Figure 9). The HVL values of the PP, PP+5% ZrO_2, PP+10% ZrO_2, and PP+15% ZrO_2 samples range from 0.0001 cm to 0.09 cm in the energy range of 0.005888-0.511 MeV, where the PE occurs predominantly. On the other hand, Compton scattering occurs predominantly between the energy levels 0.511-1.02 MeV, where HVL gets a value between 0.047 cm and 0.123 cm. Finally, pair production occurs predominantly in the high energy zone, where HVL values range from 0.123 cm to 0.489 cm. The relationship between the material thickness required to halve the incoming photon power and the incoming photon energy is clearly seen from these HVL values. Figure 8 shows that the material thickness required by the S15 sample, which is produced by adding 15% ZrO_2 ceramic material into the PP, to absorb the same photon energy is reduced to approximately half, even in the high energy region.

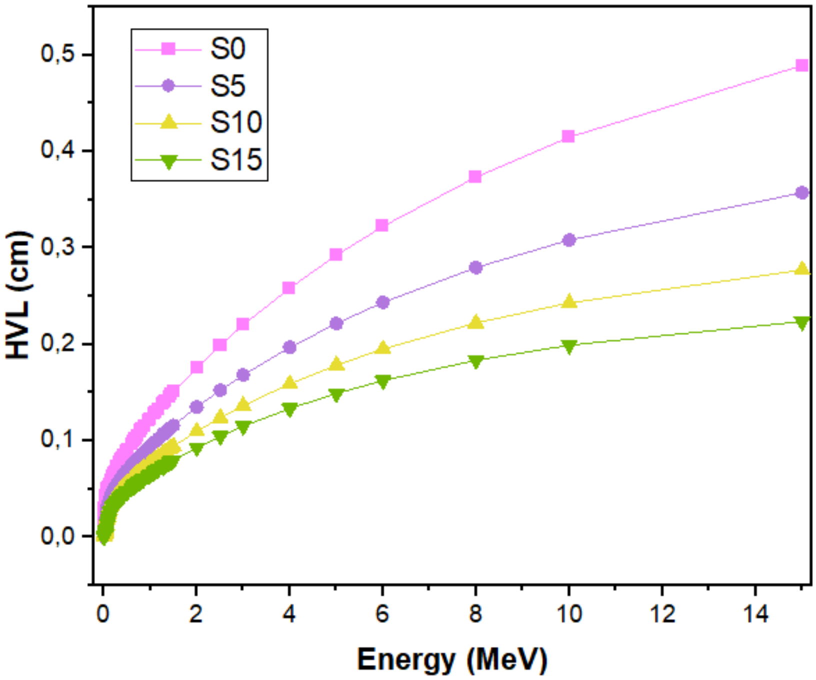

Figure 9. *HVL value of the samples*

Figure 10 shows the TVL plot, which indicates the material thick necessary to reduce the incoming radiation intensity by 90%. In this figure, it is plainly observed that the thickness values of the studied materials should be higher than their HVL values. The ^{60}Co source, which is widely used in industry, is a radioactive gamma radiation source. This gamma radiation source has various photopeaks in the energy regions where Compton scattering, PE, and pair production are predominant. When the energy level is 0.3471 MeV, the PE is dominant, and the PP, PP+5% ZrO_2, PP+10% ZrO_2, and PP+15% ZrO_2 samples have TVL values of 0.257 cm, 0.196 cm, 0.158 cm, and 0.133 cm, respectively. When the energy level is 0.8261 MeV, the Compton scattering is dominant, and the studied samples get values of 0.372 cm, 0.285 cm, 0.232 cm, and 0.196 cm, respectively. On the other hand, pair production is dominant at the energy level of 1.173 MeV, and these values are observed to be 0.441 cm, 0.338 cm, 0.276 cm, and 0.233 cm, respectively. This analysis results reveal the addition's effect on the radiation shielding material's thickness with the increase in the photon energy emitted from a radioactive source, even if the gamma sources are the same.

Figure 11 shows that the material thick required for successful two-photon interaction increases with the increase in photon energy. It is evident that the increase in ZrO_2 ceramic addition in the studied materials results in decreases in their MFP values. It is because the atomic number and density of the ZrO_2 ceramic are higher than those of the PP material. Therefore, the increase in the ZrO_2 addition results in a large number of electrons' interactions with photons. After 2 MeV, the MFP values of all the studied samples increase rapidly. This is because the LAC values of these materials become more stable after 2 MeV, and the absorption of high-energy photons decreases considerably. At the energy range 2-15 MeV, the materials PP, PP+5% ZrO_2, PP+10% ZrO_2 and PP+15% ZrO_2 have MFP ranges of 0.254 cm- 0.706 cm; 0.194 cm- 0.515 cm; 0.158 cm- 0.4 cm and 0.134 cm- 0.323 cm respectively.

GU J Sci, Part A 11(2) 407-418 (2024) 10.54287/gujsa.1475116

FNRC is a significant in terms of indicating the shielding performance of a designed material against fast neutrons. The FNRC values of the PP, PP+5% ZrO_2, PP+10% ZrO_2, and PP+15% ZrO_2 materials are 10.038 cm^{-1}, 12.651 cm^{-1}, 15.002 cm^{-1}, and 17.091 cm^{-1}, respectively. Among the four samples, the PP material has the lowest FNRC value, while the PP+15% ZrO_2 polymer matrix has the highest value (Figure 12). The density value of the PP+15% ZrO_2 polymer composite is about 95% higher than that of the PP material. Also, the FNRC value of the PP+15% ZrO_2 polymer matrix is about 70% higher than that of the PP material. The increase in the ZrO_2 ceramics addition to the PP material leads to more neutron interaction of nuclei; as a result, the FNRC values get higher figures.

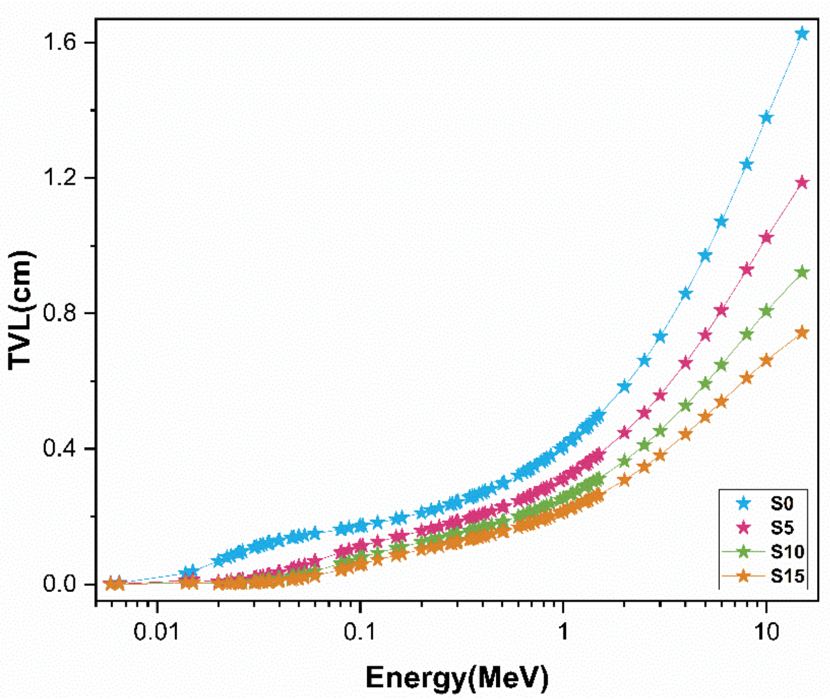

Figure 10. *TVL value of the samples*

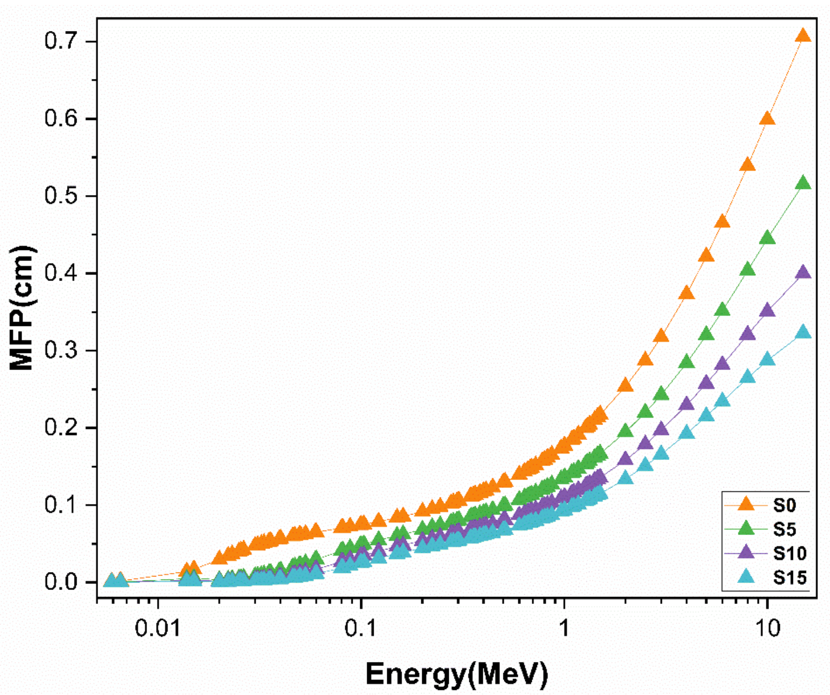

Figure 11. *MFP value of the samples*

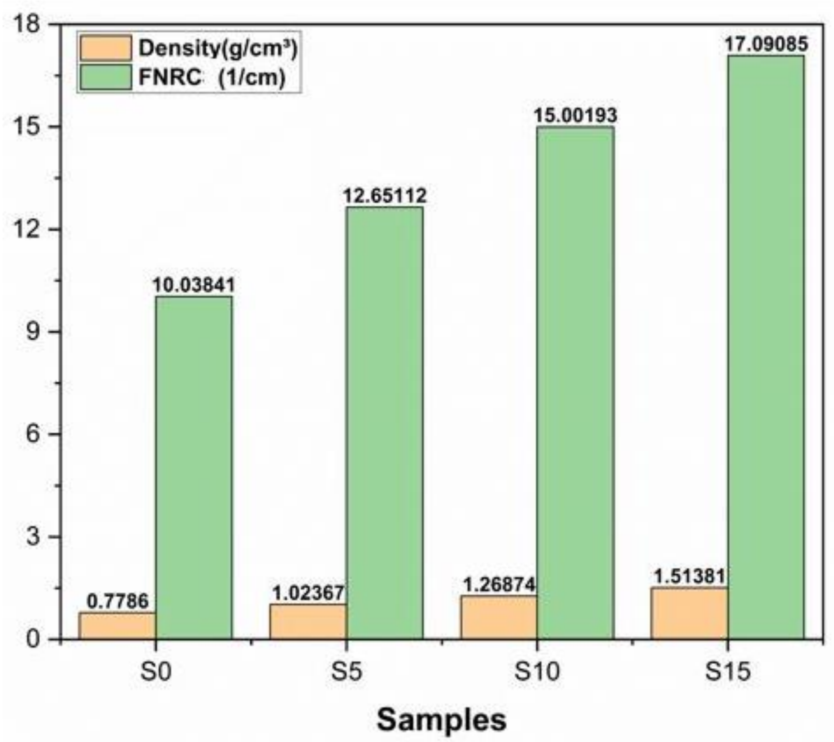

Figure 12. *FNRC and density values of the samples*

4. CONCLUSION

This study examined the radiation shielding performance of polypropylene and polymer matrix composites produced by adding ZrO_2 ceramic powder in varying proportions (5%, 10%, and 15%) to the PP material. The LAC, MAC, HVL, TVL, MFP, and FNRC, which provide significant information about gamma and neutron radiations, were analysed by utilizing the Phy-x/PSD software. Grain size and microstructures of ZrO_2 ceramic material were analyzed by SEM. Moreover, the XRD, ATR, DSC, and DTA-TG analyses were performed to obtain information about the density and characteristic properties of the PP material. Among the studied PP, PP+5% ZrO_2, PP+10% ZrO_2 and PP+15% ZrO_2 samples, PP+10% ZrO_2 had the highest LAC value while PP had the lowest LAC value. The samples with higher LAC values had lower HVL values. Therefore, the material with the highest HVL value is PP while the material with the lowest HVL value is PP+15% ZrO_2. As for the FNRC values, PP material has the lowest value (10.038 cm^{-1}) while the PP+15%ZrO_2 polymer matrix composite has the highest FNCR value (17.091 cm^{-1}). To conclude, the neutron and gamma radiation shielding features of the PP material were improved by increasing the ZrO_2 ceramic addition.

ACKNOWLEDGEMENT

The researchers would like to express their gratitude for the financial support of the Scientific Research Projects Office of Gazi University, TÜRKİYE (Project number: FKA-2023-8617), TÜBİTAK 2211-C program, and YÖK 100/2000 program.

AUTHOR CONTRIBUTIONS

Conceptualization, U.G. and Z.Ö; methodology, U.G; fieldwork, Z.Ö, S.G.A., B.Ç and E.O.; software, Z.Ö, B.Ç and E.O; title, U.G, and Z.Ö; validation, U.G., Z.Ö. and S.G.A.; laboratory work, Z.Ö, S.G.A., B.Ç and E.O.; formal analysis, U.G.; research, Z.Ö, S.G.A. and B.Ç; sources, Z.Ö and B.Ç.; data curation, Z.Ö and B.Ç.; manuscript-original draft, U.G. and Z.Ö.; manuscript-review and editing, U.G and Z.Ö; visualization, S.G.A, B.Ç and Z.Ö.; supervision, U.G; project management, U.G; funding, Gazi BAP. All authors have read and legally accepted the final version of the article published in the journal.

CONFLICT OF INTEREST

The authors declare no conflict of interest.

REFERENCES

Akinci, A. & Akbulut, H. & Yilmaz, F. (2007). The Effect of the Red Mud on Polymer Crystallization and the Interaction between the Polymer-Filler. *Polymer-Plastics Technology and Engineering*, *46*(1), 31-36. https://doi.org/10.1080/03602550600916258

Akman, F., Ogul, H., Ozkan, I., Kaçal, M. R., Agar, O., Polat, H., & Dilsiz, K. (2022). Study on gamma radiation attenuation and non-ionizing shielding effectiveness of niobium-reinforced novel polymer composite. *Nuclear Engineering and Technology*, *54*(1), 283-292. https://doi.org/10.1016/j.net.2021.07.006

Aldawood, S., Asemi, N. N., Kassim, H., Aziz, A. A., Saeed, W. S., Al-Odayni, A.-B. (2024). Gamma radiation shielding by titanium alloy reinforced by polymeric composite materials. *Journal of Radiation Research and Applied Sciences*, *17*(1), 100793. https://doi.org/10.1016/j.jrras.2023.100793

Alzahrani, J. S., Lebedev, A. V., Avanesov, S. A., Hammoud, A., Alrowaili, Z. A., Mahmoud, Z. M. M., Olarinoye, I. O., & Al-Buriahi, M. S. (2022). Synthesis and properties of tellurite based glasses containing Na_2O, BaO, and TiO_2: Raman, UV and neutron/charged particle shielding assessments. *Ceramics International*, *48*(13), 18330-18337. https://doi.org/10.1016/j.ceramint.2022.03.092

Ardiansyah, A., Heryanto, H., Armynah, B., Salah, H., Sulieman, A., Bradley, D. A., & Tahir, D. (2023). Physical, mechanical, optical, and gamma radiation shielding properties of the BaO-based glass system prepared by the melt-quench technique: A review. *Radiation Physics and Chemistry*, *210*, 111059. https://doi.org/10.1016/j.radphyschem.2023.111059

Cho, K., Li, F., & Choi, J. (1999) Crystallization and melting behavior of polypropylene and maleated polypropylene blends. *Polymer*, *40*(7), 1719-1729. https://doi.org/10.1016/S0032-3861(98)00404-2

Kamislioglu, M. (2021). Research on the effects of bismuth borate glass system on nuclear radiation shielding parameters. *Results in Physics*, *22*, 103844. https://doi.org/10.1016/j.rinp.2021.103844

Kavun, Y., Kerli, S., Eskalen, H., & Kavgacı, M. (2022). Characterization and nuclear shielding performance of Sm doped In_2O_3 thin films. *Radiation Physics and Chemistry*, 194, 110014. https://doi.org/10.1016/j.radphyschem.2022.110014

Kılıçoğlu, O., & Tekin, H. O. (2020). Bioactive glasses with TiO_2 additive: Behavior characterization against nuclear radiation and determination of buildup factors. *Ceramics International*, *46*(8-Part A), 10779-10787. https://doi.org/10.1016/j.ceramint.2020.01.088

Krylova, V. & Dukštienė, N. (2013). Synthesis and Characterization of Ag_2S Layers Formed on Polypropylene. *Journal of Chemistry*, *2013*(1), 987879. https://doi.org/10.1155/2013/987879

Labour, T., Gauthier, C., Séguéla, R., Vigier, G., Bomal, Y., & Orange, G. (2001) Influence of the β crystalline phase on the mechanical properties of unfilled and $CaCO_3$-filled polypropylene. I. Structural and mechanical characterization. *Polymer*, *42*(16), 7127-7135. https://doi.org/10.1016/S0032-3861(01)00089-1

Malidarre, R. B., Akkurt, İ., & Kavas, T. (2021). Monte Carlo simulation on shielding properties of neutron-gamma from 252Cf source for Alumino-Boro-Silicate glasses. *Radiation Physics and Chemistry*, *186*, 109540. https://doi.org/10.1016/j.radphyschem.2021.109540

Mingliang, G., Demin, J., & Weibing, X. (2007). Study on the Crystallization Properties of Polypropylene/Montmorillonite Composites. *Polymer-Plastics Technology and Engineering*, 46(10), 985-990. https://doi.org/10.1080/03602550701519449

Papageorgiou, D. G., Bikiaris, D. N., & Chrissafis, K. (2012). Effect of crystalline structure of polypropylene random copolymers on mechanical properties and thermal degradation kinetics. *Thermochimica Acta*, *543*, 288-294. https://doi.org/10.1016/j.tca.2012.06.007

Szondy, B., Bodnár, B., Grossetête, A., Gain, T., & Aszódi, A. (2024). Review of solutions developed for improving maneuvering flexibility in German, French and Russian PWRs targeting to explore future possibilities for the new VVER-1200 nuclear power plant units in Hungary. *Nuclear Engineering and Design*, *419*, 112965. https://doi.org/10.1016/j.nucengdes.2024.112965

Şakar, E., Özpolat, Ö. F., Alım, B., Sayyed, M. I., & Kurudirek, M. (2020). Phy- X / PSD: Development of a user friendly online software for calculation of parameters relevant to radiation shielding and dosimetry. *Radiation Physics and Chemistry*, *166*, 108496. https://doi.org/10.1016/j.radphyschem.2019.108496

Tyagi, G., Singhal, A., Routroy, S., Bhunia, D., & Lahoti, M. (2021). Radiation Shielding Concrete with alternate constituents: An approach to address multiple hazards. *Journal of Hazardous Materials*, *404*(Part B), 124201. https://doi.org/10.1016/j.jhazmat.2020.124201